



Correlation between Shear-Wave Velocity and Dynamic Cone Resistance for Gravelly Soil

Jashod Roy, M.ASCE¹; Kyle M. Rollins, M.ASCE²; Adda Athanasopoulos-Zekkos, M.ASCE³; and Dimitrios Zekkos, M.ASCE⁴

Abstract: Developing empirical correlations between the shear-wave velocity (V_s) and the standard penetration test (SPT) blow count has been a long-term practice for sandy, silty, and clayey soils. However, the existing correlations are not suitable for gravelly soils because the SPT is not particularly reliable for gravelly soils due to the interference of SPT sampler with relatively large-size gravel particles. Hence, in the present study, a new correlation has been developed between V_s and the dynamic cone penetration test (DPT) resistance for gravelly soils. The DPT, which consists of a 74-mm-diameter cone to reduce the interference of large particles, has recently been used to correlate the liquefaction resistance of gravelly soils. A large database has recently been developed based on both DPT and V_s data collected from different companion sites all around the world to develop new liquefaction triggering procedures. Based on this database, linear and log-linear correlations have been developed considering the effect of vertical effective stress. Results showed that the correlations among the uncorrected DPT and V_s resistance and the vertical effective stress are much stronger in comparison with the correlation obtained between the overburden-corrected DPT resistance and V_s . A reasonable agreement was observed between the measured and computed V_s for both linear and log-linear correlations. **DOI:** 10.1061/JGGEFK.GTENG-11254. © 2023 American Society of Civil Engineers.

Introduction

The small-strain shear modulus G_0 is a fundamental mechanical property of soil and is directly related to the shear-wave velocity V_s . The shear modulus (G_0) is a key soil parameter necessary for analyzing ground response, soil–structure interaction under seismic loading, and machine vibration problems. In addition, V_s has also been correlated to the liquefaction resistance of sandy soils (Kayen et al. 2013; Andrus and Stokoe 2000; Cao et al. 2011; Zhou et al. 2020) and gravelly soils (Chang 2016; Rollins et al. 2022) based on large liquefaction case history databases. Therefore, estimating V_s for any soil deposit in a reliable cost-effective manner is of great importance for geotechnical engineers.

Although the shear-wave velocity can be measured by using a variety of in situ methods, e.g., the downhole test, cross-hole test, seismic cone penetration test (CPT), multichannel analysis of surface waves (MASW), suspension logging, and so on, these methods usually require a substantial amount of additional time and expense in any project. On the other hand, data from penetration testing are routinely available for most projects; therefore, reliable correlations between V_s and penetration resistance would be very desirable.

¹Research Assistant, Dept. of Civil and Environment Engineering, Brigham Young Univ., 430 Engineering Bldg., Provo, UT 84602 (corresponding author). ORCID: https://orcid.org/0000-0003-0854-3790. Email: jashod.roy@gmail.com

²Professor, Dept. of Civil and Environment Engineering, Brigham Young Univ., 430 Engineering Bldg., Provo, UT 84602. Email: rollinsk@byu.edu

³Associate Professor, Dept. of Civil Engineering, Univ. of California, Berkeley, CA 94720. Email: adda.zekkos@berkeley.edu

⁴Associate Professor, Dept. of Civil Engineering, Univ. of California, Berkeley, CA 94720. ORCID: https://orcid.org/0000-0001-9907-3362. Email: zekkos@berkeley.edu

Note. This manuscript was submitted on August 11, 2022; approved on May 18, 2023; published online on July 14, 2023. Discussion period open until December 14, 2023; separate discussions must be submitted for individual papers. This paper is part of the *Journal of Geotechnical and Geoenvironmental Engineering*, © ASCE, ISSN 1090-0241.

Although measured values are always preferable, there is certainly a trade-off between accuracy and economics. This is particularly true when preliminary analyses must be performed within a limited budget.

To address these issues, several researchers have developed empirical correlations between the standard penetration test (SPT) blow count (N_{60}) and V_s based on both field and laboratory test data. Most of these correlations are in the functional form

$$V_s = A N^B \tag{1}$$

where A and B = constants that depend on the soil type as derived from a database for which this relation is developed. Several SPT- V_s correlations for sand have been developed (e.g., Ohta et al. 1978; Ohta and Goto 1978; Hasancebi and Ulusay 2007; Dikmen 2009), and these early correlations did not include any of the correction factors associated with SPT hammer efficiency, rod length, sample inside diameter, and even overburden pressure, as summarized by Jafari et al. (2002). Sykora and Koester (1988) found relatively poor correlation between V_s and overburden-corrected SPT blow count $(N_1)_{60}$ compared with the previously developed correlations between V_s and N_{60} . Afterward, Andrus et al. (2004) correlated overburden-corrected shear-wave velocity (V_{s1}) with overburden-corrected SPT blow count $(N_1)_{60}$ for Holocene clean sands with the following functional form:

$$V_{s1} = A(N_1)_{60}^B \tag{2}$$

The SPT- V_s correlations developed to date have primarily involved sandy, silty, or clayey deposits, although some correlations are more generic for all soil types. But these correlations would not generally be applicable for gravelly soils because the SPT is not particularly reliable for gravelly soils due to the small (51 mm) diameter of the SPT penetrometer relative to large gravel particles, which can artificially increase the penetration resistance even for loose to medium dense gravelly deposits (Cao et al. 2013).

A well-known alternative to the SPT or CPT for gravelly soils in North America is the Becker penetration test (BPT). The BPT

penetrometer is a closed-end 168-mm-diameter casing with a diameter that is intended to reduce the effect of particle size on the penetration resistance. The BPT blow count $N_{\rm BC}$ is converted to an equivalent SPT N_{60} value using correlations based on field tests (Harder and Seed 1986). Rollins et al. (1998) used equivalent SPT N_{60} values derived from BPT testing and cross-hole shearwave velocity tests at gravel sites to develop correlations between shear-wave velocity and equivalent SPT blow counts for gravelly soils and found better prediction of V_s using blow counts uncorrected for overburden pressure along with vertical effective stress as a second independent variable.

The dynamic cone penetration test (DPT) is an alternative penetrometer that was developed in China to characterize gravelly soil (Cao et al. 2013). The DPT equipment consists of a 74-mm-diameter cone tip attached to a 60-mm-diameter drill rod continuously driven by a 120-kg hammer with a free fall height of 100 cm. With a 74-mm-diameter cone tip, the DPT is significantly larger than the SPT and reduces the effect of interference with gravel particles. In addition, the smaller-diameter drill rod reduces the loss in energy due to rod friction. Recently, DPT has been used to correlate the liquefaction resistance of gravelly soil based on a gravel liquefaction case history database from different sites around the world (Cao et al. 2013; Rollins et al. 2021).

Geophysical investigations have also been performed at many sites where gravels have and have not liquefied throughout the world. For example, Andrus and Stokoe (2000) made velocity measurements at gravel liquefaction sites in Idaho to correlate the liquefaction resistance of gravelly soils with V_s . Cao et al. (2011) developed direct correlations between the liquefaction resistance and V_{s1} based on gravel liquefaction case history data at the Chengdu plain in China. Recently, the V_s database for gravel liquefaction case histories has been expanded by performing in situ V_s tests at various gravel liquefaction sites around the world and Rollins et al. (2022) developed a new probabilistic liquefaction triggering procedure for gravelly soil based on V_{s1} . Although there have been several investigations to characterize the liquefaction potential of gravelly soil, no specific correlation between the V_s and DPT penetration resistance has been developed for gravelly soil to date.

In the newly collected DPT and V_s databases for gravelly soils reported by Cao et al. (2011, 2013) and Rollins et al. (2021, 2022), there were many sites where V_s measurements were conducted near companion DPT boreholes to characterize the same gravelly deposit by two different methods. Hence, in this study, these companion DPT and V_s test results from the database of Cao et al. (2011, 2013) and Rollins et al. (2021, 2022) have been collected to investigate potential correlations between V_s and the DPT penetration resistance. Details regarding both the DPT and V_s data collection along with the regression procedure to develop the DPT- V_s correlation are described in the following sections.

Collection of DPT and V_s Data

As reported by Cao et al. (2013) and Rollins et al. (2021), the DPT was performed at various gravelly sites around the world where gravelly soil did or did not liquefy during past earthquake events and the DPT resistance (N_{120}) has been correlated with liquefaction potential of gravelly soil. The DPT blow count, N_{120} , indicates the number of hammer blows required to drive the DPT cone 30 cm with a 120-kg hammer dropped from a height of 1 m. As standardized by the Chinese Design Code (2001), raw DPT blow counts are collected at every 10 cm of penetration and multiplied by three to get the equivalent N_{120} for 30 cm of penetration to maintain

consistency with the SPT drive length as well as preserve the 10-cm detail in the penetration profile (Cao et al. 2013).

Based on 1,200 hammer energy measurements, Cao et al. (2013) found that the Chinese DPT provided an average of 89% of the theoretical hammer free-fall energy ($E_{\rm Chinese\,DPT}$) at sites on the Chengdu plain in China. Rollins et al. (2021) performed DPT soundings at most sites using the standard Chinese hammer energy (120 kg weight and 1 m drop) or by performing companion DPT tests with both the Chinese hammer energy and SPT hammer energy (63.5 kg weight and 0.76 m drop). The hammer energy transferred to the drill rods was measured by a pile-driving analyzer (PDA) device at each respective location. Because the energy delivered by a given hammer ($E_{\rm Hammer}$) in the study of Rollins et al. (2021) was likely different from the energy transferred by a Chinese DPT hammer ($E_{\rm Chinese\,DPT}$), energy correction was made using the simple linear reduction suggested by Seed et al. (1985) for SPT testing as follows:

$$N_{120} = N_{\text{Hammer}} \cdot (E_{\text{Hammer}} / E_{\text{Chinese DPT}})$$
 (3)

where $N_{\rm Hammer}$ = number of blows per 0.3 m of penetration obtained with a hammer transferring an energy of $E_{\rm Hammer}$ to the drill rods and $E_{\rm Chinese\,DPT}$ is the 89% of the theoretical free-fall energy provided by the Chinses DPT.

In addition, Cao et al. (2013) recommend an overburden correction factor, C_N , to obtain the normalized N'_{120} value using the following equation:

$$N_{120}' = N_{120}C_N \tag{4}$$

where

$$C_N = (100/\sigma'_{vo})^{0.5} \le 1.7$$
 (5)

where σ'_o = initial vertical effective stress (kN/m²). In the current study, a limiting value of 1.7 was included to be consistent with the C_N used to correct penetration resistance from other in situ tests (Youd et al. 2001).

Thus, by applying the energy and overburden correction on the raw blow counts, both N_{120} and N'_{120} versus depth profiles were produced by Cao et al. (2013) and Rollins et al. (2021) for all the DPT investigation sites.

On the other hand, geophysical tests were also performed by Cao et al. (2011) and Rollins et al. (2022) at various liquefaction and no-liquefaction gravelly sites around the world to correlate the liquefaction potential of gravelly soil with V_s . Among all the sites investigated by Cao et al. (2011, 2013) and Rollins et al. (2021, 2022), a total of 54 sites where companion DPT and V_s tests were performed at the same locations within a distance of 1 to 6 m have been considered in the present study, as listed in the Supplemental Materials. Among these 54 locations, there are 48 sites where V_s data were obtained using the MASW method conducted in just the forward direction. At the remaining six sites, V_s profiles were obtained by performing other types of in situ measurements. As presented in the Supplemental Materials, the spectral analysis of surface wave (SASW) method (Andrus 1994) was used to obtain V_s data at the sites at Pence Ranch, Larter Ranch, and Whiskey Springs in Idaho. At a site in L'Aquila, Italy, a downhole (DH) test was used to obtain V_s data, and at one site in Avasinis, Italy, the V_s profile was obtained by a cross-hole (CH) test.

The MASW method considers the dispersion of Rayleigh waves to generate an apparent phase-velocity dispersion relationship that is then used in an inversion analysis to derive a V_s profile. MASW surveys were typically performed, as described by Rollins et al. (2022), using a linear array at each site composed of vertical

geophones (4.5 Hz) typically spaced at 1-m intervals to increase resolution near the surface and at 3-m intervals for greater depths. A sledgehammer (usually 5.5. kg) striking on a plastic plate was used as the seismic source. The source was aligned to the geophones and located at several offsets (three to five) for each linear array. For each offset, a stack of three to five measurements was considered adequate to increase the signal-to-noise ratio.

The recorded phase offset of different frequency waves (f-k analysis) was used to develop a relationship between phase velocity and frequency (or wavelength), called a dispersion curve. Based on the dispersion curves, inversion analyses were conducted using the Park et al. (1999) methodology and typically without a priori subsurface information to derive a shear-wave velocity model. It is well known that major differences in interpretation arise not from the dispersion analyses particularly, but from the inversion algorithm used to estimate the V_s profile from the dispersion curve. Therefore, the inversion process has a much stronger influence over the final V_s model compared with the dispersion curve generation method (Garofalo 2016). More details regarding the inversion procedure used for various sites have been given by Rollins et al. (2022).

The V_s values obtained by various surface-wave and in situ methods were corrected for overburden pressure to obtain V_{s1} using the following equation:

$$V_{s1} = V_s (P_a / \sigma'_{vo})^{0.25} \tag{6}$$

where σ'_{vo} = initial vertical effective stress; and P_a = atmospheric pressure approximated by a value of 100 kPa as suggested by Sykora (1987) and adopted by Youd et al. (2001). These normalized V_{s1} profiles and the original V_s profiles were then plotted as a function of depth for all the boreholes reported by Cao et al. (2011) and Rollins et al. (2022).

As a part of the present study, the DPT N_{120} profiles and their paired V_s profiles along with other relevant information about the soil profiles (groundwater table, total stress, and effective stress) have been collected. Then, for each of these boreholes, average N_{120} and effective stress (σ'_v) has been calculated for each layer portion, through which the corresponding V_s is interpreted to be constant. Thus, N_{120} , V_s , and σ'_v sets at different depths from each borehole have been obtained. The number of these sets depends on the number of stair steps identified in the V_s profile where average N_{120} and σ'_v were also obtained for each interval.

Paired N_{120} , V_s , and σ'_v values have been obtained only for the gravelly soil layers. At some locations in Italy (Avasinis, Bordano, and L'Aquila), there are several thin silty and sandy layers, which are reflected by various peaks and troughs in the DPT profiles, but the V_s profiles remain constant along the depth. Part of the reason behind this discrepancy can be that the in situ V_s methods often estimate the V_s of a large volume of soil strata, and hence thin layers at the exact location of the DPT might not have been captured in the V_s profiles. For these locations, average N_{120} , V_s , and σ'_v values have been obtained only for the critical gravelly layers excluding the thin soil deposits to reduce the error while developing correlation among these parameters. Critical gravelly layers indicate those layers most likely to trigger and manifest liquefaction at the ground surface. Typically, these are the layers with the lowest average DPT or V_s resistance below the groundwater table but near the ground surface. Critical layers have been selected over an interval of 1 m or more representative N_{120} or V_{s1} that is less affected by thin peaks or troughs.

The values of N_{120} , V_s , and σ'_v from all the companion boreholes are summarized in the Supplemental Materials, along with some other relevant features of each site. The overburden-corrected DPT blow count (N'_{120}), and V_{s1} values computed for each borehole have

also been included in the Supplemental Materials. In total, 242 data points have been collected from 54 different sites, among which 150 data points come from China and the remaining 92 data points come from other parts of the world. Although a large portion of these data (64%) come from the Chengdu plain of China, this database is comprised of a variety of gravelly deposits including natural deposits from alluvial fans, glacial outwash, fluvial, and glaciofluvial deposits as well as human-made fills at ports and dams.

In this database, the maximum depth is typically about 15 m and the maximum vertical effectives stress, σ'_v , is about 250 kPa. These deeper layers are mostly from the sites in Alaska and a few sites in China. The N_{120} values ranged from 2 to 55 and Vs values typically ranged from about 100 to 400 m/s. Using the correlations to extrapolate beyond these ranges should be done with appropriate caution. This range of V_s (most less than 200 m/s and nearly all less than 300 m/s) is relatively low compared with the V_s range of 300 to 900 m/s reported by Foti et al. (2018) for gravelly soil. One likely reason for this is that many of these soil deposits were relatively loose and hence liquefied during a seismic event. Therefore, they would be expected to have lower V_s values. In addition, the gravelly soils at sites investigated by Cao et al. (2011, 2013) and Rollins et al. (2021, 2022) were primarily comprised of sandy gravel or a gravelly sand mixture where sand contents are in the range of 30%-70%. So those gravelly deposits with substantial sand contents might produce V_s values more in the range of sandy soil than that of clean gravelly soil.

Development of Correlations between DPT Penetration Resistance and Shear-Wave Velocity

Based on the database reported in the Supplemental Materials, correlations can be developed between the DPT blow count (N_{120}) and shear-wave velocity (V_s) for gravelly soil. In this context, the influence of overburden pressure (σ'_v) can be considered in two ways: (1) by transforming N_{120} and V_s to N'_{120} and V_{s1} using Eqs. (3) and (4) prior to the regression analysis, or (2) by performing the statistical regression considering σ'_v as an independent variable along with N_{120} and V_s . These two approaches were previously adopted in developing some SPT blow count- V_s correlations (Rollins et al. 1998; Brandenberg Scott et al. 2010) and hence similar procedures have been followed in the present study.

Although, the SPT blow count- V_s correlations are primarily based on log-linear combinations of N_{60} , V_s , and σ'_v or $(N_1)_{60}$ and V_{s1} , in this study, both linear and log-linear combinations of N_{120} , V_s , and σ'_v or N'_{120} and V_{s1} have been considered to investigate the performance of different variations. All these regressions were performed by using the JMP Pro 16 commercial program (SAS Institute Inc. 2021; Youd and Noble 1997). Results of all these regression outcomes are summarized in the following sections.

Linear Correlation between V_{s1} and N'₁₂₀

To obtain the correlation between V_{s1} and N'_{120} , the N_{120} and V_s values have first been converted to N'_{120} and V_{s1} , as shown in the Supplemental Materials, by using Eqs. (4) and (6), respectively. Based on these N'_{120} and V_{s1} values, the equation for V_{s1} , given by

$$V_{s1} = 180.34 + 3.23N_{120}' \tag{7}$$

has been obtained by linear regression analysis. The p-values for all the regression variables were less than 0.0001, and the F-ratio of the regression model was 172.81. However, the correlation coefficient (R^2) for this regression equation was found to be 0.436 with a

root-mean square error of 0.39. These statistics clearly indicate a poor correlation between N'_{120} and V_{s1} .

Log-Linear Correlation between V_{s1} and N'_{120}

In this regression, the logarithm of V_{s1} and N'_{120} has been considered. The correlation obtained by this approach provides the following equation for V_{s1} :

$$V_{s1} = 121.51 \left(N_{120}' \right)^{0.238} \tag{8}$$

The *p*-values for all the regression variables were less than 0.0001, and the *F*-ratio of the regression model was 159.24. The correlation coefficient (R^2) for this correlation was 0.409 with a root-mean square error of 0.17. Therefore, the correlation between N'_{120} and V_{s1} was found to be consistently weak for both the linear and log-linear combinations.

Linear Correlation among V_s , N_{120} , and σ'_v

In this approach, both the uncorrected N_{120} and the effective overburden pressure (σ'_v) have been considered as independent variables for predicting the uncorrected V_s . Based on a linear regression, the following equation for V_s has been obtained:

$$V_s = 108.25 + 3.66N_{120} + 0.642\sigma_v' \tag{9}$$

The p-values for all the regression variables were less than 0.0001, and the F – ratio of the regression model was 318.47. The regression coefficient (R^2) for this correlation was 0.724, with a root-mean square error of 0.34. Clearly, the consideration of σ'_v as a separate independent variable has significantly improved the correlation coefficient compared with the previous approaches of correcting N_{120} and V_s for overburden pressure prior to the regression.

Log-Linear Correlation among V_s , N_{120} , and σ'_v

In this trial, a regression analysis has been performed using the logarithms of V_s , N_{120} , and σ'_v with the logarithms of N_{120} , and σ'_v as the independent variables to obtain the following correlation equation for V_s :

$$V_s = 40.44(N_{120})^{0.242} (\sigma'_{\nu})^{0.24} \tag{10}$$

The p-values for all the regression variables were less than 0.0001, and the F-ratio of the regression model was 293.2. In this case, the correlation coefficient (R^2) was found to be 0.674 with a root-mean square error of 0.16. Interestingly, the regression indicates that the exponent of the vertical effective stress was 0.24, which is close to the value of 0.25 that is known to describe the influence of effective stress on shear-wave velocity for granular soils in general, as well as gravelly soils in particular (Menq 2003; Hubler et al. 2017) as indicated in Eq. (6).

Although the regression correlation coefficient in the log-linear regression was somewhat lower compared with the linear regression, the correlation was still significantly stronger than the correlations provided by using the overburden-corrected values based on Eqs. (7) and (8). The correlation coefficients for V_s , based on N_{120} and σ_v^r [Eqs. (9) and (10)], were similar to several existing correlations developed between V_s and SPT N_{60} values for sandy soils. For example, Dikmen (2009) obtained a correlation between uncorrected V_s and N with a correlation coefficient (R^2) of 0.72 based on 82 borehole samples of sand. Hasancebi and Ulusay (2007) also obtained a correlation between uncorrected V_s and V_s with a correlation coefficient of 0.65 for sandy soil. Ohta and Goto (1978) found different correlations between V_s and V_s for different soil

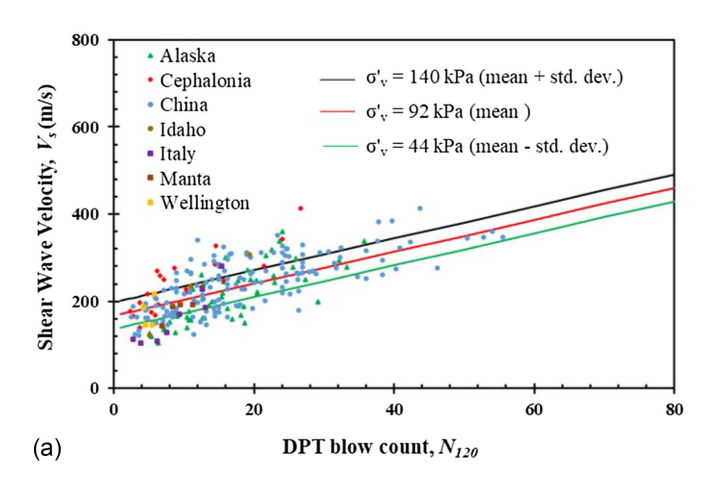
types including the effect of soil depth and geologic epoch. These correlation coefficients varied from 0.72 to 0.86 for different soils, among which one correlation for sandy soil was found to be 0.72.

Although, the correlations developed for gravelly soil based on the DPT and V_s database would not be directly comparable with the existing V_s and SPT-N correlations for sandy soil, the range of correlation coefficients indicates that a reasonable correlation has been developed for gravelly soil based on the database of DPT N_{120} and V_s values.

Relative Influence of N_{120} and σ_{v}' on the Correlation with V_{s}

Based on the correlations developed in Eqs. (9) and (10), the trend lines of V_s versus N_{120} and V_s versus σ_v' for both linear and log-linear correlations have been plotted in Figs. 1 and 2, respectively along with all the data points reported in the Supplemental Materials. Multiple regression lines have been obtained in both V_s versus N_{120} and V_s versus σ_v' plots for the multiple values of σ_v' and N_{120} , respectively. In this study, the mean and mean \pm one standard deviation values of σ_v' (92 \pm 48 kPa) and N_{120} (15 \pm 10 blows/0.3 m) have been considered to obtain the regression lines in each plot and provide a fair comparison regarding the relative influence of the two variables.

The plots corresponding to the linear correlation in Fig. 1 show that the influence of N_{120} on V_s in Fig. 1(b) was slightly more than



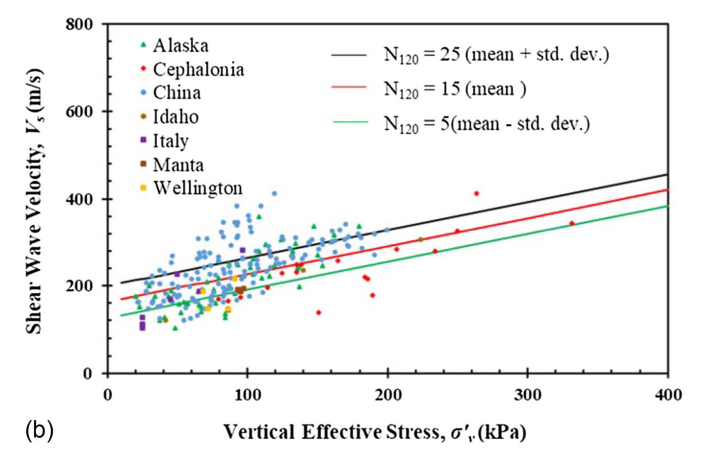


Fig. 1. Variation of (a) V_s versus N_{120} for the mean and mean \pm one standard deviation values of σ'_v ; and (b) V_s versus σ'_v for the mean and mean \pm one standard deviation values of N_{120} for the linear correlation model.

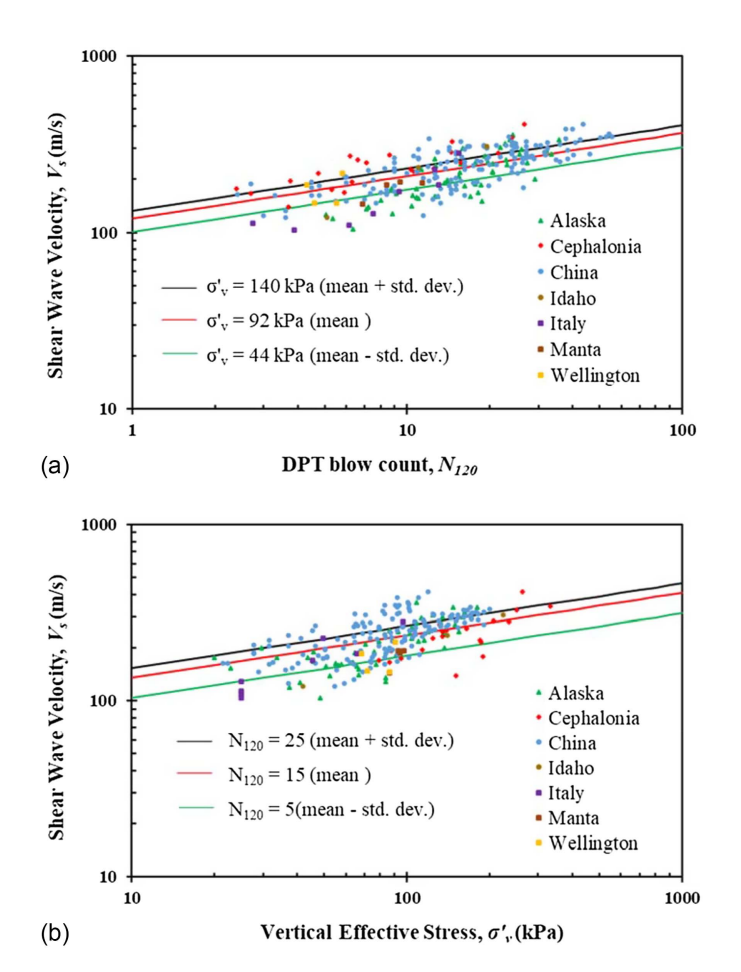


Fig. 2. Variation of (a) V_s versus N_{120} for the mean and mean \pm one standard deviation values of σ'_v ; and (b) V_s versus σ'_v for the mean and mean \pm one standard deviation values of N_{120} for the log-linear correlation model.

the influence of σ'_v on V_s in Fig. 1(a) because the spread between different N_{120} lines was slightly more in the V_s versus σ'_v plot than the spread between various σ'_v lines in the plot of V_s versus N_{120} . For example, considering the mean N_{120} of 15, the corresponding V_s took the values of 222, 189, and 255 m/s for the mean and mean \pm one standard deviation values of σ'_v , i.e., 92, 44, and 140 kPa. On the other hand, for the mean σ'_v of 92 kPa, the corresponding V_s attained the values of 222, 187, and 258 m/s for the mean and mean \pm one standard deviation N_{120} values of 15, 5, and 25. Clearly, these values indicate that the influence of N_{120} on V_s is a little more than the influence of σ'_v on V_s .

The plots corresponding to the log-linear correlation in Fig. 2 depict similar behavior in the V_s versus N_{120} and V_s versus σ'_v plots as that observed for the linear correlation. For the mean N_{120} of 15, the corresponding V_s took the values of 192, 231, and 257 m/s for three different values of σ'_v , i.e., 44, 92, and 140 kPa, whereas for the mean σ'_v of 92 kPa, the corresponding V_s attained the values of 185, 232, and 258 m/s for the N_{120} values of 5, 15, and 25.

Therefore, the V_s of gravelly soil is governed slightly more by N_{120} compared with σ'_v , although the difference was not substantial. This can be explained by the fact that the V_s of any gravelly stratum would depend more on the density of the soil matrix in that stratum than the effective overburden pressure produced by the overlying soil strata. This fact is also supported by the plots of Figs. 1 and 2, where the points on the V_s versus σ'_v plot were more unevenly scattered (specifically between σ'_v of 80 to 120 kPa), in

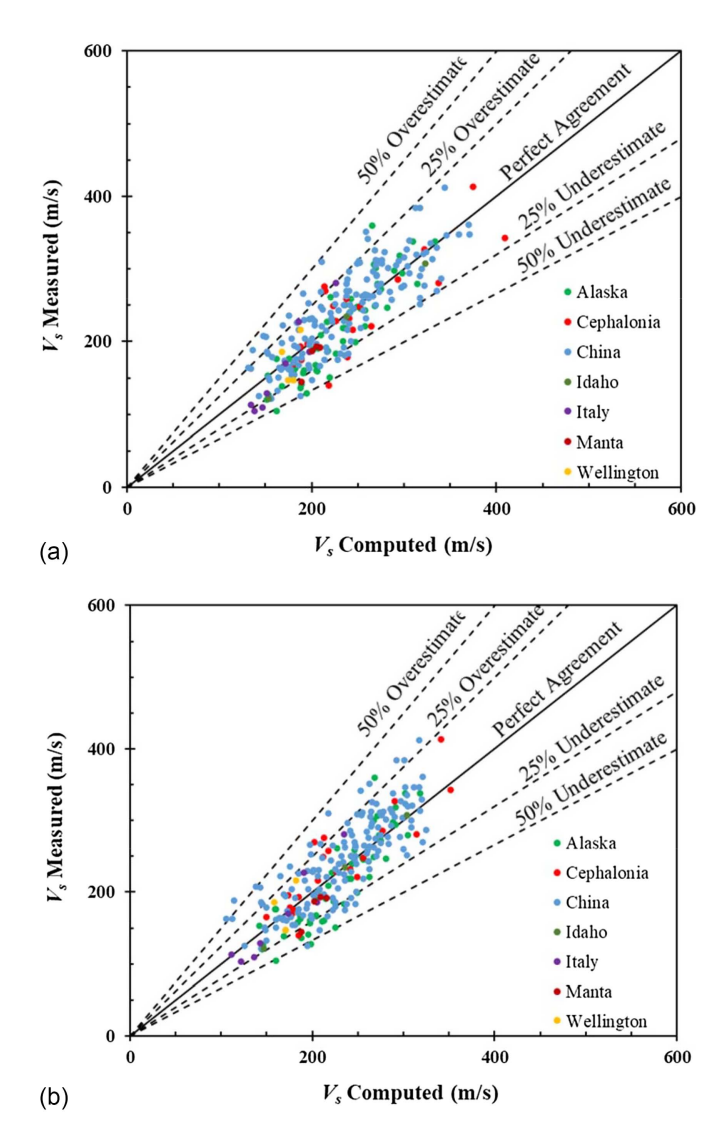


Fig. 3. Comparison between the measured and computed V_s values for (a) linear; and (b) log-linear models developed in the present study.

comparison with the points on the V_s versus N_{120} plot, indicating that the correlation between V_s and N_{120} is a bit stronger than the correlation between V_s and σ'_v .

Figs. 1 and 2 (both V_s versus N_{120} and V_s versus σ'_v plots) showed a certain amount of scatter, as indicated by the standard root-mean square error values of 0.34 and 0.17 for the linear and log-linear model, respectively. This range of errors is similar to the range of 0.29 obtained by Brandenberg Scott et al. (2010) for V_s versus N_{60} correlations for sands.

One major reason behind the scatter in Fig. 3, or even in Figs. 1 and 2, is the use of different methods of determining V_s at different sites of the world. Different methods can produce different V_s profiles at different depths because they use different ranges of wave frequency and soil volumes in each method (Brandenberg Scott et al. 2010). Moreover, geophysical measurements sample a large volume of soil to yield an average V_s profile for a particular soil layer and do not often capture the local variations, which are usually captured by the typical penetration test methods such as the SPT or CPT. On the other hand, the penetration test results were considered as point measurements for each borehole, and spatial averaging of penetration resistance was required to define the whole soil layer and may also contribute some uncertainty in the overall site characterization.

Relative Influence of Geological Origin on V_s Correlations

In addition to the regression analysis of the entire database, individual regressions have also been performed for different types of gravelly deposits viz. alluvial, man-made and fluvial or glaciofluvial deposits. In the current database, the sites in China, Idaho and Italy (Avasinis) primarily consist of alluvial deposits. The ports of Manta in Ecuador, Wellington in New-Zealand and Cephalonia (Lixouri and Argostoli) in Greece provided data for human-made gravelly fill. The sites at L'Aquila in Italy and the sites of Alaska consisted of fluvial and glacio-fluvial deposits. The resulting correlation equations for human-made fill, alluvial fan, and fluvial deposits are provided in Eqs. (11)–(16) along with their respectively correlation coefficients. The *p*-values for all the variables in each equation were found to be less than 0.0001.

Linear Correlations

The linear correlation for human-made deposits is calculated as follows:

$$V_s = 117.25 + 5.396N_{120} + 0.396\sigma'_v; \quad R^2 = 0.79$$
 (11)

The linear correlation for alluvial deposits is calculated as follows:

$$V_s = 115.99 + 3.28N_{120} + 0.696\sigma_v'; \quad R^2 = 0.73$$
 (12)

The linear correlation for fluvial deposits is calculated as follows:

$$V_s = 70.78 + 4.284N_{120} + 0.81\sigma'_v; \quad R^2 = 0.75$$
 (13)

Log-Linear Correlations

The log-linear correlation for human-made deposits is calculated as follows:

$$V_s = 31.37(N_{120})^{0.215}(\sigma'_v)^{0.305}; \quad R^2 = 0.76$$
 (14)

The log-linear correlation for alluvial deposits is calculated as follows:

$$V_s = 46.52(N_{120})^{0.23} (\sigma'_{r})^{0.22}; \quad R^2 = 0.70$$
 (15)

The log-linear correlation for fluvial deposits is calculated as follows:

$$V_s = 26.79 \times (N_{120})^{0.386} (\sigma'_v)^{0.225}; \quad R^2 = 0.73$$
 (16)

The regression analyses show that the equation for human-made fill produced the highest correlation coefficient of about 0.79, whereas the correlation correlations for the alluvial and fluvial deposits were 0.73 and 0.75, respectively, for the linear correlation. On the other hand, the regression coefficients for the log-linear correlations were 0.79, 0.69, and 0.76 for the human-made, alluvial, and fluvial deposits, respectively. Hence, in all cases, accounting for the geological origin of the gravelly deposits yielded somewhat higher correlation coefficients than the general correlations in Eqs. (9) and (10). This result is reasonable and consistent with results of regression analyses correlating V_s with N_{60} values obtained from BPT reported by Rollins et al. (1998).

Comparison between the Measured and Computed V_s

To compare the performance of both the linear and log-linear correlations, the V_s values computed by Eqs. (9) and (10) have been

plotted versus the corresponding measured V_s values for all the sites, as shown in Figs. 3(a and b). In addition, the perfect agreement line along with the 25% and 50% overestimate and underestimate lines are shown.

It can be observed that the linear correlation in Fig. 3(a) gives somewhat better agreement between the measured and computed values compared with the log-linear correlation in Fig. 3(b). The statistics indicate that approximately 83% of the data points fell within the $\pm 25\%$ error bound lines and 98% of the data fell within $\pm 50\%$ error bound lines in Fig. 3(a). But, the 25% and 50% error bounds in Fig. 3(b) contained approximately 82% and 97% of the data, respectively. The difference between the linear and log-linear correlations are relatively minor, which has already been indicated by the very similar regression coefficients for the data in Figs. 1 and 2. However, the overall data set in Fig. 3(b) for the log-linear model still seems to be slightly skewed with respect to the perfect agreement line, whereas the data set in Fig. 3(a) seems to be more evenly distributed, indicating less skewness or bias with respect to the perfect agreement line. Therefore, the linear correlation is recommended for the gravelly soils based on the database collected in the present study.

Summary and Conclusions

A large database consisting of 242 data pairs with DPT penetration resistance (N_{120}) and shear-wave velocity (V_s) in gravelly deposits at the same depth has been collected. The data came from a variety of countries and geological environments. Using the data set, statistical regressions have been performed to develop correlations between V_s and DPT penetration resistance.

Correlations have been developed between (1) the overburden-corrected shear-wave velocity (V_{s1}) and the overburden-corrected DPT penetration resistance (N'_{120}) , and (2) the uncorrected shear-wave velocity (V_s) and the uncorrected DPT penetration resistance (N_{120}) along with the effective vertical effective stress (σ'_v) . The second approach with the effective overburden pressure as an independent variable produced a better regression model with a higher correlation coefficient $(R^2 = 0.72 \text{ versus } R^2 = 0.44)$.

Both linear and log-linear combinations have been evaluated, and the linear correlation appears to have somewhat better predictive capability in comparison with the log-linear model, although both are acceptable. In the linear correlation, 83% of the data points fell within 25% of the predicted value, and 98% of the data points fell within 50% error bound lines. In contrast, the same 25% and 50% error bounds contained 82% and 97% data points in the log-linear model. Correlation coefficients improved by 7 to 12 percentage points when regression equations were developed using data with similar geologic origin, consistent with previous reports by Rollins et al. (1998) for gravels and Brandenberg Scott et al. (2010) for sands.

Investigation of the relative effect of effective overburden pressure (σ'_v) and DPT resistance (N_{120}) on the variation of V_s showed that σ'_v had a little more influence on the variation of V_s compared with N_{120} , although the difference was not substantial. This observation is consistent with observations made by Brandenberg Scott et al. (2010) for the correlation among V_s , N_{60} , and σ'_v for sands.

Limitations of the Present Study

In the present data set, the depth of gravelly soil strata where DPT blow count and V_s data have been collected was within 1–15 m below the ground surface, and the corresponding effective stress was in the range of 20–330 kPa. No data were collected beyond

15 m depth with higher overburden stress. Therefore, the empirical correlations developed in this study should be applicable within shallow depths (0–15 m) but not necessarily for the deeper gravelly strata.

Secondly, in the current database, 29 datapoints came from human-made fills. The remaining 213 datapoints came from natural soils (alluvial, fluvial, and glaciofluvial deposits) among which 122 datapoints were for liquefaction sites and 91 datapoints were from no-liquefaction sites. Hence, most datapoints in the reported database were from natural soil deposits Geologic factors such as formation of soil deposits, aging, cementation, stress, and strain history may significantly govern the microstructure of the soil matrix and eventually can have substantial impact on the in situ measurement of $V_{\rm s}$.

Lastly, the V_s data in the present database were in the range of 100-530 m/s among which 80% of the data fall below 300 m/s. Similarly, the DPT N_{120} blow counts are in the range of 2–55 where almost 80% of the data fall below the blow count of 25. Hence, the current database primarily consists of loose to medium dense gravelly soil with a few datapoints corresponding to dense gravelly strata. But the denser gravelly soil, which consist of relatively large gravel particles, can produce a substantially higher range of V_s (300–900 m/s), and the correlations developed in the present study may not necessarily be appropriate for dense gravelly strata. Also, the DPT resistance can be affected due to the interference with large gravel particles; Meyerhof (1957) stated that all penetration tests become unreliable if the maximum particle size approaches the diameter of the penetrometer or the sampler spoon. However, further investigation is still required to specifically quantify the effect of particle size on DPT.

Data Availability Statement

Some or all data, models, or code that support the findings of this study are available from the corresponding author upon request.

Acknowledgments

Funding for this study was provided by Grant No. G16AP00108 from the US Geological Survey Earthquake Hazard Reduction Program and Grant Nos. CMMI-1663546 and CMMI-16632884 from the National Science Foundation. This funding is gratefully acknowledged. However, the opinions, conclusions, and recommendations in this paper do not necessarily represent those of the sponsors.

Supplemental Materials

Table S1 is available online in the ASCE Library (www ascelibrary.org).

References

- Andrus, R. D. 1994. "In situ characterization of gravelly soils that liquefied in the 1983 Borah Peak earthquake." Ph.D. dissertation, Dept. of Civil Engineering, Univ. of Texas at Austin.
- Andrus, R. D., P. Piratheepan, B. S. Ellis, J. Zhang, and C. H. Juang. 2004. "Comparing liquefaction evaluation methods using penetration-VS relationships." *Soil Dyn. Earthquake Eng.* 24 (9–10): 713–721. https://doi.org/10.1016/j.soildyn.2004.06.001.

- Andrus, R. D., and K. H. Stokoe II. 2000. "Liquefaction resistance of soils from shear-wave velocity." *J. Geotech. Eng.* 126 (11): 1015–1025. https://doi.org/10.1061/(ASCE)1090-0241(2000)126:11(1015).
- Brandenberg Scott, J., N. Bellana, and T. Shantz. 2010. "Shear wave velocity as function of standard penetration test resistance and vertical effective stress at California bridge sites." Soil Dyn. Earthquake Eng. 30 (10): 1026–1035.
- Cao, Z., T. L. Youd, and X. Yuan. 2011. "Gravelly soils that liquefied during 2008 Wenchuan, China Earthquake, Ms=8.0." Soil Dyn. Earthquake Eng. 31 (8): 1132–1143. https://doi.org/10.1016/j.soildyn.2011.04.001.
- Cao, Z., T. L. Youd, and X. Yuan. 2013. "Chinese dynamic penetration test for liquefaction evaluation in gravelly soils." *J. Geotech. Geoenviron. Eng.* 139 (8): 1320–1333. https://doi.org/10.1061/(ASCE)GT.1943-5606 .0000857.
- Chang, W. J. 2016. "Evaluation of liquefaction resistance for gravelly sands using gravel content-corrected shear-wave velocity." J. Geotech. Eng. 142 (5): 04016002. https://doi.org/10.1061/(ASCE)GT.1943-5606 0001427.
- Chinese Design Code. 2001. *Design code for building foundation of Chengdu region*. DB51/T5026-2001. Chengdu, China: Administration of Quality and Technology.
- Dikmen, Ü. 2009. "Statistical correlations of shear wave velocity and penetration resistance for soils." J. Geophys. Eng. 6 (1): 61–72. https://doi.org/10.1088/1742-2132/6/1/007.
- Foti, S., C. Comina, D. Boiero, and L. V. Socco. 2009. "Non-uniqueness in surface wave inversion and consequences on seismic site response analyses." *Soil Dyn. Earthquake Eng.* 29 (6): 982–993. https://doi.org/10.1016/j.soildyn.2008.11.004.t.
- Garofalo, F., et al. 2016. "Inter PACIFIC project: Comparison of invasive and non-invasive methods for seismic site characterization. Part I: Intracomparison of surface wave methods." Soil Dyn. Earthquake Eng. 82 (3): 222–240. https://doi.org/10.1016/j.soildyn.2015.12.010.
- Harder, L. F., and H. B. Seed. 1986. Determination of penetration resistance for coarse-grained soils using the Becker hammer drill. Rep. No. UCB/EERC-86/06. Berkeley, CA: Earthquake Engineering Research Center
- Hasancebi, N., and R. Ulusay. 2007. "Empirical correlations between shear wave velocity and penetration resistance for ground shaking assessments." *Bull. Eng. Geol. Environ.* 66 (2): 203–213. https://doi.org/10 .1007/s10064-006-0063-0.
- Hubler, J. F., A. Athanasopoulos-Zekkos, and D. Zekkos. 2017. "Monotonic, cyclic, and postcyclic simple shear response of three uniform gravels in constant volume conditions." *J. Geotech. Geoenviron. Eng.* 143 (9): 04017043. https://doi.org/10.1061/(ASCE)GT.1943-5606.0001723.
- Jafari, M. K., A. Shafiee, and A. Razmkhah. 2002. "Dynamic properties of fine-grained soils in south of Tehran." J. Seismol. Earthquake Eng. 4 (1): 25–35.
- Kayen, R., R. E. S. Moss, E. M. Thompson, R. B. Seed, K. O. Cetin, A. Der Kiureghian, Y. Tanaka, and K. Tokimatsu. 2013. "Shear-wave velocitybased probabilistic and deterministic assessment of seismic soil liquefaction potential." *J. Geotech. Eng.* 139 (3): 407–419. https://doi.org/10 .1061/(ASCE)GT.1943-5606.0000743.
- Menq, F. Y. 2003. Dynamic properties of sandy and gravelly soils. Austin, TX: Univ. of Texas.
- Meyerhof, G. G. 1957. "Discussion on research on determining the density of sands by spoon penetration testing." In *Proc., 4th Int. Conf. on Soil Mechanics and Foundation Engineering*. London: Butterworths.
- Ohta, Y., and N. Goto. 1978. "Empirical shear wave velocity equations in terms of characteristic soil indexes." *Earthquake Eng. Struct. Dyn.* 6 (2): 167–187. https://doi.org/10.1002/eqe.4290060205.
- Ohta, Y., N. Goto, H. Kagami, and K. Shiono. 1978. "Shear wave velocity measurement during a standard penetration test." *Earthquake Eng. Struct. Dyn.* 6 (1): 43–50. https://doi.org/10.1002/eqe.4290060106.
- Park, C. B., R. D. Miller, and J. Xia. 1999. "Multichannel analysis of surface waves." *Geophysics* 64 (3): 800–808. https://doi.org/10.1190/1.1444590.
- Rollins, K. M., M. Evans, N. Diehl, and W. Daily. 1998. "Shear modulus and damping relationships for gravels." J. Geotech. Geoeviron. Eng. 124 (5): 396–405.

- Rollins, K. M., J. Roy, A. Athanasopoulos-Zekkos, D. Zekkos, S. Amoroso, and Z. Cao. 2021. "New dynamic cone penetration test-based procedure for liquefaction triggering assessment of gravelly soils." J. Geotech. Geoenviron. Eng. 147 (12): 13. https://doi.org/10.1061/(ASCE)GT.1943-5606.0002686.
- Rollins, K. M., J. Roy, A. Athanasopoulos-Zekkos, D. Zekkos, S. Amoroso, Z. Cao, G. Millana, M. Vassallo, and G. Di Giulio. 2022. "A new Vs-based liquefaction triggering procedure for gravelly soils." J. Geotech. Geoenviron. Eng. 148 (6): 04022040. https://doi.org/10.1061/(ASCE)GT.1943-5606.0002784.
- SAS Institute, Inc. 2021. *JMP*® *Pro 16: Data analysis software for mac and windows*, 1989–2021. Cary, NC: SAS Institute, Inc.
- Seed, H. B., K. Tokimatsu, L. F. Harder, and R. M. Chung. 1985. "Influence of SPT procedures in soil liquefaction resistance evaluations." *J. Geotech. Eng.* 111 (12): 1425–1445. https://doi.org/10.1061/(ASCE) 0733-9410(1985)111:12(1425.

- Sykora, D. W. 1987. Creation of a data base of seismic shear wave velocities for correlation analysis. Vicksburg, MI: Waterways Experiment Station.
- Sykora, D. W., and J. P. Koester. 1988. "Review of existing correlations between shear wave velocity or shear modulus and standard penetration resistance in soils." In *Proc., Earthquake Engineering and Soil Dynamics II Conf.*, 389–404. Reston, VA: ASCE.
- Youd, T. L., et al. 2001. "Liquefaction resistance of soils: Summary Report from the 1996 NCEER and 1998 NCEER/NSF Workshops on evaluation of liquefaction resistance of soils." *J. Geotech. Eng.* 127 (4): 297–313. https://doi.org/10.1061/(ASCE)1090-0241(2001)127:10(817).
- Youd, T. L., and S. K. Noble. 1997. "Liquefaction criteria based on statistical and probabilistic analyses." In *Proc.*, *NCEER Workshop on Evaluation of Liquefaction Resistance of Soils*, 201–205. Buffalo, NY: State Univ. of New York.
- Zhou, Y. G., P. Xia, D. S. Ling, and Y. M. Chen. 2020. "Liquefaction case studies of gravelly soils during the 2008 Wenchuan earthquake." Eng. Geol. 274 (2): 105691. https://doi.org/10.1016/j.enggeo.2020.105691.